Study of benzophenone grafting on reduced graphene oxide by unconventional techniques

Journal Name

RSCPublishing

ARTICLE

Study of benzophenone grafting on reduced graphene oxide by unconventional techniques

Cite this: DOI: 10.1039/xoxxoooooox

Ignazio Roppolo[a†*], Annalisa Chiappone[a†], Samuele Porro[a], Micaela Castellino[a], Enzo Laurenti[b]

Received ooth January 2012,
Accepted ooth January 2012

DOI: 10.1039/xoxxoooooox

www.rsc.org/

Understanding the mechanisms acting behind the functionalization of graphene is of paramount importance for the application of functionalized graphene in polymeric nano-composite materials. This work reports the study of the influence of benzophenone in a UV-mediated grafting process on graphene oxide, carried out by unconventional spectroscopic techniques, such as electron spin resonance and thermogravimetric analysis coupled with in-situ infra-red spectroscopy. Using these techniques, a direct investigation of the grafting was achieved for the first time, while up to now only indirect evidences were provided, opening new perspectives for the study of small molecules grafting on graphene sheets. The presence of benzophenone grafted on reduced graphene oxide surface was demonstrated, and in particular an unstable radical species attributable to the semipinacol radical of benzophenone was revealed, which is a key step of the functionalization process. Moreover, X-ray photoelectron spectroscopy demonstrated that the grafting process effectively reduced graphene oxide recovering the properties of graphene, contemporarily leaving active sites for a further polymer functionalization.

Introduction

The functionalization of graphene sheets with polymeric macromolecules is a research field that has attracted increasing interest in the last decade.[1] This process was proved to be of fundamental importance in the fabrication of graphene/polymer composites,[2-4] a new class of materials that are considered to be very promising for application in electronics and sensing.[5, 6]
One of the most promising approaches for a massive production of polymer-functionalized graphene is the chemical modification of graphene oxide (GO).[7-12] GO is generally produced on large scale from graphite through a well-established oxidative mechanism,[13] it is commercially available and relatively cheap.[14] Moreover, due to the presence of intrinsically labile oxygen groups on the surface and at the edges of GO sheets, it is relatively easy to attach and chemically bond polymer chains, or to recover graphene-like properties through reduction processes with the aim of obtaining reduced graphene oxide (RGO).[14-16] Many approaches have been proposed in the literature for polymer grafting of GO[7-12, 17, 18] and to processes focusing on GO reduction to RGO,[19-25] but little attention was so far devoted to achieve these two stages contemporarily.
In a previous work, we have recently proposed a UV-mediated functionalization mechanism, with the purpose of synthesizing a polymer-grafted RGO, using benzophenone as a radical intermediate for GO reduction and to achieve further functionalization of RGO sheets.[26] This process demonstrated to be fast, easy to implement and adaptable to a great variety of monomer functionalities. The grafting procedure was demonstrated to be extremely reliable and repeatable, however, in order to have direct proof of the benzophenone grafting, a further investigation focused on the interaction between graphene and benzophenone (BP) needs to be implemented.
Electron Spin Resonance (ESR) is a useful technique for the characterization of paramagnetic systems, such as free radicals and transition metal ions. Moreover, it is able to detect single occupancy of energy levels in the band gap of semiconducting materials, therefore it is normally employed in the characterization of defects. However, several studies on amorphous carbon show that ESR can detect states that are not necessarily recombination centers but also, for instance, mid-gap states due to π bonding in sp^2 coordinated clusters.[27] In addition, ESR was demonstrated to give useful information in the characterization of carbon-based nanostructured materials, for example in the investigation of dopants content[28] and defects localization[29] in synthetic nanocrystalline diamond films, in the study of surface adsorption and functionalization of carbon nanotubes[30] and more recently in the investigation of the presence of various functionalities at the edges of graphene nanoribbons.[31, 32] Consequently, ESR is expected to give an insight in the characterization of the radical species that are generated during the UV-mediated functionalization of graphene using benzophenone intermediates.

In addition to ESR characterization of benzophenone-functionalized graphene, in the present work the interaction of benzophenone with GO sheets was also investigated through thermogravimetric analysis (TGA) coupled with in-situ infra-red (IR) spectroscopy. The presence of benzophenone grafted to RGO sheets was thus demonstrated and investigated by direct experiments, while usually indirect evaluations such as weight increase or TGA drop weight are reported in the literature.[33-35] X-ray photoelectron spectroscopy (XPS) was used to confirm the reduction of GO during the functionalization process. Non-conventional techniques such as ESR and TGA coupled with in-situ IR revealed to be very promising for a comprehensive characterization of the GO chemistry and the surface functionalization mechanisms.

Results and Discussion

In a previous experiment[26] we proposed a novel dual-step procedure for reduction and functionalization of GO, which involved as fundamental step the UV irradiation of a GO solution in the presence of BP. It is well known in the literature that BP, when UV irradiated, is able to abstract an extractable hydrogen atom from the environment creating semipinacol radicals.[33, 36] In our recent work we demonstrated that the BP abstraction of hydrogen atoms from GO surfaces induced a spontaneous reduction of GO to RGO, with following recovery of many properties of graphene such as increased conductivity and hydrophobicity. Moreover, we proposed that during this step some semipinacol radicals could recombine with latent radicals on the RGO surface, inducing the grafting of these molecules. It was then demonstrated that during a second step these bonds could act as starting points for the grafting of acrylic and methacrylic monomers.

Even if the whole mechanism was confirmed by conventional structural, morphological, and electrical characterization,[26] a deep investigation of the interaction between semipinacol groups and RGO surfaces by specific spectroscopic techniques remained a challenge in order to give an insight of the GO surface chemistry and its functionalization.

First, the effect of the amount of BP on the GO reduction process was investigated with the purpose of optimizing the process parameters. Different amounts of BP (1, 3 and 5 wt/wt in comparison to the amount of GO) were added to the GO dispersion in DMF and UV irradiated for 5 minutes. The obtained samples were analyzed by XPS and TGA. The XPS survey spectra of pristine GO before and after UV irradiation and of the three samples containing BP revealed the presence of carbon and oxygen only at the sample surfaces (ESI Figures S1 to S5). Figure 1 shows the XPS spectra of C1s peaks, deconvoluted using Gaussian-Lorentz functions, while backgrounds have been removed with Shirley function.[37] The C1s peak is composed of three contributions: the main due to C-C/C-H bond (peak I), the second due to C-O bond (peak II) and the third due to –C=O bond (peak III).[38] The data confirmed the crucial role of BP in the reduction process, since a nearly complete reduction was obtained even at low BP concentration, as indicated by the evident decrease of peaks II and III in the treated samples. The importance of the presence of BP in the process is clear by comparing the data with the sample simply UV-irradiated. However, based only on XPS experiments, it is difficult to evaluate the influence of the increasing amount of BP on the reduction of GO, since the relative intensities of the different contributions to C1s peak are quite similar for all BP concentrations and they could be attributed both to grafted semipinacol radicals and unreduced GO.

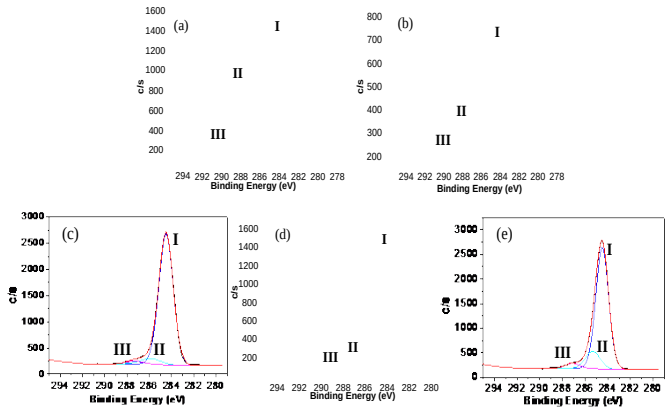

Figure 1. XPS spectra of pristine GO (a), GO after 5 minutes of UV irradiation (b), and GO after 5 minutes of UV irradiation in the presence of different amounts of BP: 1/1 wt (c), 1/3 wt (d) and 1/5 wt (e).

In order to better investigate the reduction level of RGO sheets, TGA experiments were conducted (Figure 2). The degradation curve of pristine GO shows a main degradation step at 220°C that is attributed to the pyrolysis of the labile oxygen-containing functional groups. After UV–irradiation (GO-UV sample) a fairly strong decrease of the main degradation temperature was observed. We suppose that the unreduced species on the sheets, also revealed by XPS (Figure 1b), present modified thermal stability in comparison to the oxidized groups on pristine GO, thus decomposing at lower temperatures. When the BP- treated samples are considered, unfortunately, the degradation of BP (around 180°C) overlaps the drop of weight of the partially reduced graphene oxide (GO-UV). It is therefore difficult to distinguish exactly the contribution of semipinacol grafted on the surface and the unreduced groups. However, TGA measurements confirmed that increasing the amount of BP the maximum of the degradation peak shifts towards the degradation temperature of BP (190 °C)[26], indicating an increasing importance of this degradation mechanism. Moreover, a higher residual was found with 5 wt/wt of BP at the end of the experiment, indicating an increase of reduced part of graphene oxide. These observations can clarify the results obtained by XPS, confirming that the peak II (C-O) did not show any significant variation among samples treated with increasing amount of BP because of the simultaneous GO-reduction (decrease of C-O groups) and BP grafting (addition of C-O groups on the RGO surface). It can be thus concluded that increasing the amount of BP results in a more complete reduction of GO and more successful grafting.

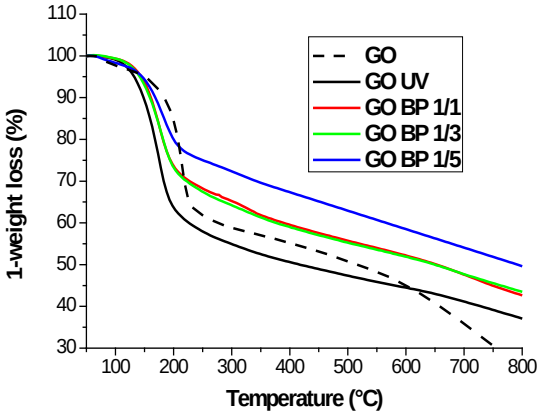

Figure 2. TGA curves of pristine GO, GO after UV irradiation and GO after UV irradiation in the presence of different amounts of BP.

In order to deeply study the degradation process and to address the drop of weight with the presence of semipinacol groups grafted on the surface, TGA experiments coupled with FT-IR were performed. The GO sample with 1/5 wt BP was chosen for this measurement, as it is the one that showed a higher degree of reduction (Figure 2). Figure 3 reports a comparison of the FT-IR spectra of GO, GO/UV and GO/BP 1/5 wt at the main degradation temperature (220, 175 and 190°C respectively). The GO spectrum shows a large presence of peaks between 2000 cm^{-1} and 1300 cm^{-1} which are related to the degradation of the oxygen-containing species; the same peaks are also visible in the GO/UV and GO/BP spectra, indicating the persistence of functionalities even after the UV treatment. Moreover, it is important to evidence that GO/BP shows a peak at 1400 cm^{-1} that could be correlated to the degradation of the aromatic groups in BP (ESI, Figure S6). This peak is not present in degradation spectra of GO/UV and GO, clearly suggesting the presence of grafted BP onto the partially reduced GO. Finally, both UV irradiated samples (GO/UV and GO/BP) present some peak that could be associated to the evaporation of residual DMF used as solvent during the reduction and grafting processes: an increase of carbonyl group at 1740 cm^{-1} and a small peak at 1100 cm^{-1} (ESI, Figure S7).

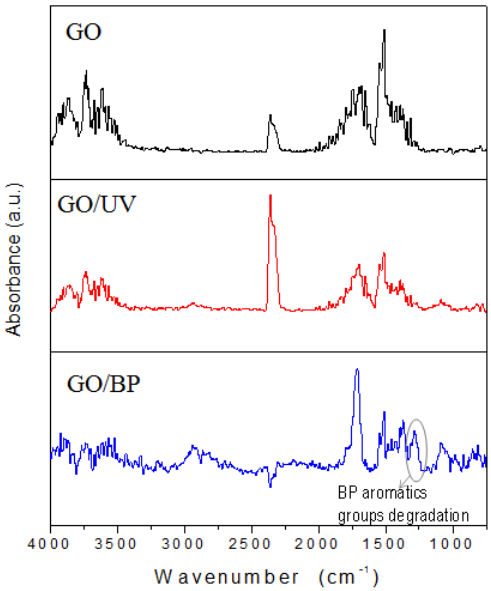

Figure 3. IR on line spectra during TGA of GO, GO after 5 minutes of irradiation (GO/UV) and GO after 5 minutes of irradiation in the presence of BP 1/5 wt (GO/BP).

In order to further confirm the presence of semipinacol groups, ESR experiments were conducted at room temperature on GO, GO/UV and GO/BP (1/5wt) samples re-dispersed in DMF and placed in quartz capillary tubes. Since ESR spectroscopy allows to detect and characterize the free radicals present in the analyzed dispersion, all the samples were further UV irradiated in order to generate new radical species. In fact, after the first BP grafting procedure, it is possible to homolytically break the bond between the semipinacol group (BP) and the GO surface by means of a second UV irradiation, thus generating radicals both on graphene surface and in solution as semipinacol radicals. [26, 33, 39]

After 2 minutes of UV irradiation, the ESR spectra of GO, GO/UV and GO/BP samples were recorded as previously described. The ESR spectra of all samples show the presence of a single isotropic signal at g = 2.003, similar to those previously observed by Huo and co-workers[40] and assigned to an open-shell phenalenyl-like radical on the basis of a previous study about graphene fragments.[41] As described by Huo and co-workers, the signal is present both in irradiated and non irradiated GO samples and its intensity increases with the irradiation time, confirming the progressive reduction of GO to RGO by UV light. Moreover, in our experiments, the highest concentration of radical species was observed for the GO/BP sample, probably due to the previous irradiation to which the sample has been subjected during the functionalization process.

Since we were not able to observe directly the presence of semipinacol or other unstable radicals, even if irradiating the sample in situ, a different approach was developed. In order to stabilize the unstable radicals that were possibly generated, an appropriate amount of the spin trap DMPO was added to the different GO samples before the treatment under the UV lamp and the ESR spectra were recorded after 2 min of irradiation time. Under these conditions, more complex and intense ESR spectra with a common g-factor equal to 2.001 have been recorded (Figure 4) due to the formation of different adducts between DMPO and the radical species generated during the

irradiation of the samples. Each different spectral pattern can be associated to different radical species generated by UV-irradiation of materials and solvent, and stabilized by the presence of the spin trap.

Analyzing the data in Figure 4, it clearly appears that both the GO/UV and GO/BP ESR spectra are similar to the spectra of the solvent (DMF) and probably due to the presence of an adduct between DMPO and a radical species of DMF generated by UV light (DMPO-DMF)[42]. Furthermore, the spectrum of GO/BP also shows the presence of a weak pattern of lines, partially hidden by the DMPO-DMF signal. The position of the only two visible lines of this pattern (marked by arrows in Figure 4) coincide with the outer lines of the spectrum of a DMPO-BP stable radical species obtained when a solution of BP in DMF is irradiated in the presence of DMPO (lower spectrum in Figure 4, the six lines corresponding to the DMPO-BP radical adduct are highlighted).

In order to better explain these signals, simulations with the software WinSIM36 were made and the calculated parameters are summarized in Table 1. On the basis of the best results of the simulations, the ESR spectrum of GO/BP results to be the sum of four different species: I, a single isotropic signal, observed also in absence of DMPO as described above; II, the DMPO-DMF species; III, the DMPO-BP radical adduct; IV, a three-lines pattern of a nitroxide-like radical, probably due to a degradation of DMPO as a results of irradiation.

With the aim of confirming the presence of a spectral pattern attributable to BP radical species, the same experiments were repeated by using water instead of DMF as solvent for GO. In these conditions a different spectral pattern is obtained, consisting of narrower lines that facilitate both the simulation and the interpretation of results. The EPR spectra were recorded and simulated as previously and the results of the calculation are also shown in Table 1.

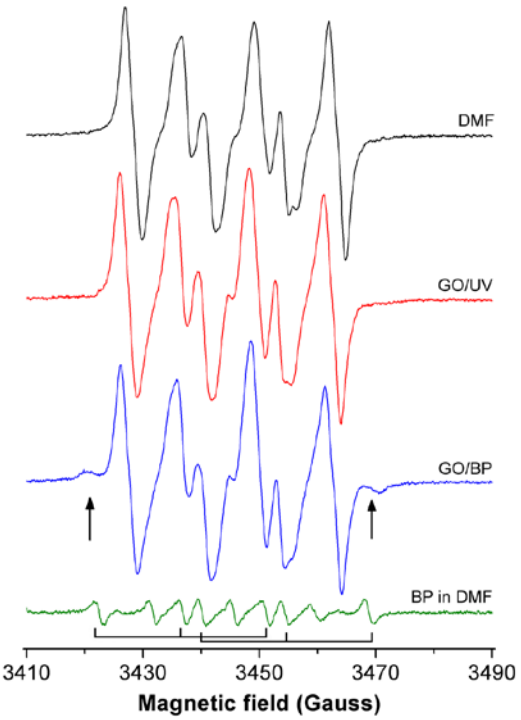

Figure 4. ESR spectra of GO/UV and GO/BP samples with DMPO in DMF compared with the spectra of solvent and BP alone. In the spectra of BP in DMF, the six lines corresponding to the DMPO-BP radical adduct are highlighted.

Table 1. Parameters calculated by simulation with WinSIM software of the ESR experiments. For each species resulting from the simulation process (see the text for details), the relative abundance (%) and the hyperfine separation constants for nitrogen (aN) or β-hydrogen (aH) DMPO nuclei were reported when they are present.

		I	II			III			IV		
Sample	**Solvent**	**%**	**%**	**aN**	**aH**	**%**	**aN**	**aH**	**%**	**aN**	**corr.**
	DMF		100.0	12.83	9.26						0.986
GO/UV	DMF	7.4	92.6	12.87	9.17						0.992
GO/BP	DMF	4.9	90.0	12.83	9.12	2.7	14.54	17.32	2.4	18.55	0,993
BP	DMF		11.2	13.88	10.22	60.3	14.31	17.68	28.5	13.93	0,969
BP*	DMF						14.30	17.37			
	H_2O		100.0	14.81	15.01						0,990
GO/UV	H_2O	60.9	5.8	14.89	14.77				33.3	16.08	0,991

GO/BP	H_2O	51.1	5.6	14.91	14.70	6.5	15.97	21.38	36.8	16.13	0,985

* data from the literature[43]

In Figure 5 the experimental and simulated spectra of GO/BP in water after UV irradiation are reported as example. Also in this case the experimental spectrum can be completely simulated as the sum of four radical species: the isotropic single-line signal of GO (I, marked with an arrow); the typical four-lines pattern of the DMPO-OH adduct (II, each line is indicated with a #); a six-lines pattern attributable to the DMPO-BP adduct in water (III, indicated with *); the three-lines pattern of a nitroxide-like radical previously observed as product of degradation of DMPO in water[43, 44] (IV, indicated with §). By subtraction of the simulated components I, II and IV from the experimental spectrum of Figure 5, the presence of the DMPO-BP radical adduct becomes clearly evident (ESI, Figure S8).

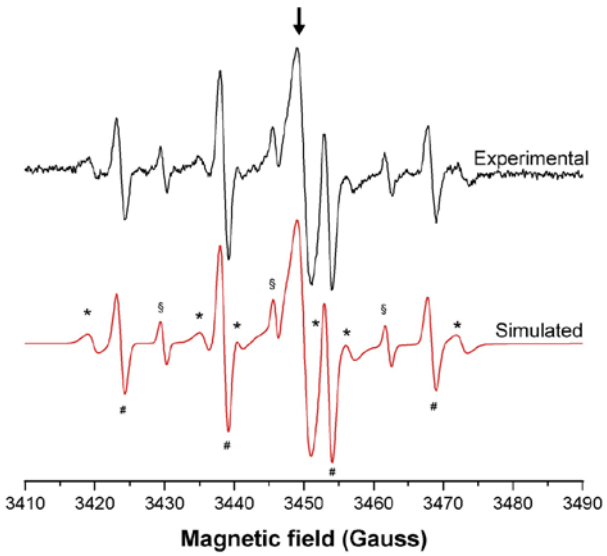

Figure 5. Experimental and simulated ESR spectra of GO/BP in water. The lines corresponding to the different adducts with DMPO are indicated as follows: I, the single-line species typical of GO and RGO (arrow); II, DMPO-OH (#); III, DMPO-BP (*); IV, the degradation product (§).

The difficulty to obtain a direct observation of the spectrum of semipinacol, due both to the low concentration of BP present on the GO samples and the instability of the radical, did not allow a direct evidence of the mechanism of GO grafting. Nevertheless the ESR data obtained with the spin trapping technique clearly revealed that, during the UV-irradiation, the GO samples are involved in the formation of different radical species. Moreover, in the case of GO/BP sample, the irradiation leads to the detachment from RGO of a few amount of BP as a radical, that is trapped by DMPO and revealed by ESR. These results are in good agreement with the previous observations, in fact all the performed experiment evidenced that the presence of BP induced an increase of the GO reduction under UV irradiation. Moreover, the recombination of semipinacol radicals on the RGO surface was directly demonstrated by ESR and IR/TGA experiments.

Conclusions

The interaction between GO and BP under UV irradiation was investigated. Combining the indications obtained from XPS and TGA experiments, it was possible to infer that by increasing the amount of BP in the initial suspension, a more complete degree of reduction was achieved. Moreover, the presence of BP grafted on the RGO surface was demonstrated by IR analysis coupled with TGA experiments and ESR spectroscopy. IR spectra showed the presence of peaks corresponding to BP while ESR revealed an unstable radical species attributable to the semipinacol radical of BP. The application of unconventional techniques for GO surface chemistry was demonstrated to be useful for a deep investigation of the functionalization, and in general opened new perspectives for the study of small molecules grafting.

Experimental

Materials

Commercial GO (thickness 0.7–1.2 nm) was purchased from Cheap Tubes Inc. (USA) and used without further purification. Benzophenone (BP, Sigma-Aldrich) was used as reducing and anchoring agent. Dimethylformamide DMF and Ethanol were used as solvents for mechanistic studies on the formation of aminoxyl radicals.

Functionalization process

10 mg of GO in DMF (0.5 mg/ml solution) were placed in a 100 ml three-necked flask. The mixture was treated in ultrasonic bath until a homogeneous dispersion was obtained. Different amounts of BP powder were then added to the dispersion, which was magnetically stirred and degassed by bubbling with nitrogen for 30 minutes. The mixture was UV irradiated with a medium-pressure mercury lamp with an intensity of 40 mW/cm^2 (Hamamatsu LC8 equipped with 8 mm light guide) while stirring at room temperature for 5 minutes. After the reaction, the solution was transferred into centrifuge tubes and centrifuged at a speed of 5000 rpm for 30 minutes. The precipitates were washed with ethanol and centrifuged several times in order to remove the unreacted BP and byproducts. The purified product was dried overnight in vacuum at 60°C.

Characterization methods

A PHI 5000 Versaprobe II Scanning X-ray Photoelectron Spectrometer (monochromatic Al K-alpha X-ray source with 1486.6 eV energy, 15 kV voltage and 1 mA anode current), was used to investigate surface chemical composition. A spot size of 100 μm was used in order to collect the photoelectron signal for both the high resolution (HR) and the survey spectra. Different pass energy values were employed: 187.85 eV for survey spectra and 23.5 eV for HR peaks. All samples were analyzed with a combined electron and argon ion gun neutralizer system in order to reduce the charging effect during the measurements. The semi-quantitative atomic compositions were obtained using Multipak 9.1 dedicated software.

Thermogravimetric analysis (TGA) was performed with a Netzsch TG 209 F1 Libra equipment instrument. All samples were previously maintained 30 minutes at 100°C in order to eliminate adsorbed water and then heated between 100°C and 800°C at a heating rate of 10°C/min in nitrogen flow of 60 ml/min. Afterwards a purge flow of nitrogen was used (20 ml/min). For control of the measurements as well as for data acquisition, NETZSCH PROTEUS 32-bit Software is employed with Advanced Software packages like c-DTA (calculated DTA-signal), Super-Res (rate-controlled mass change) and Thermokinetics. For the measurement of the temperature-dependent mass changes including gas analysis the NETZSCH TG 209 F1 Libra was simultaneously coupled to a BRUKER Optics FTIR. Data exchange between NETZSCH PROTEUS software and Bruker OPUS software is done online during the measurement. The gases evolved by thermal analysis are transferred into the IR spectrometer from Bruker Optics. The gas cell is heated to 200 °C and possesses a volume of 5.8 mL. The DTGS detector of the FT infrared spectrometer covers a rage of 500 cm^{-1} to 6000 cm^{-1}. Every spectrum is averaged from 16 scans. One scan takes around one second.
ESR spectra were recorded with an ESP 300E X-band spectrometer (Bruker). Samples, in powder or in suspension, were placed in a capillary quartz tubes or a quartz flat cell and analyzed at room temperature. Typical ESR parameters were set as follows: microwave frequency 9.69 GHz; microwave power 10 mW; modulation frequency 100 KHz; modulation amplitude 1 Gauss; time constant 40 msec; gain 1×105. ESR spectra were calculated by the WinSIM simulation program[45] (produced and distributed by NIEHS - Public EPR Software Tools). The samples were analyzed as dispersed and after two minutes of UV irradiation under a medium-pressure mercury lamp (Hamamatsu LC8) with an intensity of 50 mW/cm^2.
The g-factors were calculated by using strong pitch Bruker as reference standard (g = 2.0028) or determined by the simulation program.

Materials preparation for characterization

TGA experiments were conducted on as-synthesized dried samples. For XPS all solid samples were dispersed in water (concentration 0.5 mg/ml) in ultrasonic bath for 30 minutes, then slowly deposited by drop casting on a silicon wafer heated to 50°C in order to produce a homogenous layer. For ESR measurements, solid samples of GO were dispersed in DMF or water as described above (concentration 0.5 mg/ml) and placed in quartz capillary tubes. When needed, a small amount of the spin trap 5,5'-dimethyl-1-pirroline-N-oxide (DMPO, Sigma-Aldrich), final concentration 25 mM, was added to the sample.

Acknowledgements

The authors would like to gratefully thank Dr. Chiara Baldini from NETZSCH Gerätebau GmbH and Dr. Carolin Fischer from NETZSCH Gerätebau GmbH- Applications Laboratory for their help in IR/TGA experiments.

Notes and references

[a] Istituto Italiano di Tecnologia, Center for Space Human Robotics, C.so Trento 21, 10129 Torino, Italy Tel. :+390110903421; Fax: :+390110903401; Email address: ignazio.roppolo@iit.it.

[b] Dipartimento di Chimica, Università di Torino, Via P. Giuria 7, 10125, Torino, Italy.

† These authors contributed equally to this work.

Electronic Supplementary Information (ESI) available: XPS survey spectra, IR spectra of DMF and BP and ESR experimental and simulated data of DMPO-BP. See DOI: 10.1039/b000000x/

1. J. Liu, J. Tang and J. J. Gooding, Journal of Materials Chemistry, 2012, 22, 12435-12452.
2. T. Kuilla, S. Bhadra, D. Yao, N. H. Kim, S. Bose and J. H. Lee, Progress in Polymer Science, 2010, 35, 1350-1375.
3. S. Villar-Rodil, J. I. Paredes, A. Martinez-Alonso and J. M. D. Tascon, Journal of Materials Chemistry, 2009, 19, 3591-3593.
4. S. Stankovich, D. A. Dikin, G. H. B. Dommett, K. M. Kohlhaas, E. J. Zimney, E. A. Stach, R. D. Piner, S. T. Nguyen and R. S. Ruoff, Nature, 2006, 442, 282-286.
5. C. Soldano, A. Mahmood and E. Dujardin, Carbon, 2010, 48, 2127-2150.
6. Y. Zhu, S. Murali, W. Cai, X. Li, J. W. Suk, J. R. Potts and R. S. Ruoff, Advanced Materials, 2010, 22, 3906-3924.
7. H. Yang, F. Li, C. Shan, D. Han, Q. Zhang, L. Niu and A. Ivaska, Journal of Materials Chemistry, 2009, 19, 4632-4638.
8. S. Niyogi, E. Bekyarova, M. E. Itkis, J. L. McWilliams, M. A. Hamon and R. C. Haddon, Journal of the American Chemical Society, 2006, 128, 7720-7721.
9. Z. Liu, J. T. Robinson, X. Sun and H. Dai, Journal of the American Chemical Society, 2008, 130, 10876-10877.
10. H. Yang, C. Shan, F. Li, D. Han, Q. Zhang and L. Niu, Chemical Communications, 2009, 0, 3880-3882.
11. S. Stankovich, R. D. Piner, S. T. Nguyen and R. S. Ruoff, Carbon, 2006, 44, 3342-3347.
12. G. G. Paula Marques, Sandra Cruz, Nuno Almeida, Manoj Singh, José Grácio and António Sousa Functionalized Graphene Nanocomposites, Advances in Nanocomposite Technology, 2011.
13. W. S. Hummers and R. E. Offeman, Journal of the American Chemical Society, 1958, 80, 1339-1339.
14. D. R. Dreyer, S. Park, C. W. Bielawski and R. S. Ruoff, Chemical Society Reviews, 2010, 39, 228-240.
15. S. Pei and H.-M. Cheng, Carbon, 2012, 50, 3210-3228.
16. R. Giardi, S. Porro, A. Chiolerio, E. Celasco and M. Sangermano, Journal of Materials Science, 2013, 48, 1249-1255.
17. L. Kan, Z. Xu and C. Gao, Macromolecules, 2010, 44, 444-452.
18. K. Song, X. Zhao, Y. Xu and H. Liu, J Mater Sci, 2013, 48, 5750-5755.
19. S. Stankovich, D. A. Dikin, R. D. Piner, K. A. Kohlhaas, A. Kleinhammes, Y. Jia, Y. Wu, S. T. Nguyen and R. S. Ruoff, Carbon, 2007, 45, 1558-1565.
20. G. Wang, J. Yang, J. Park, X. Gou, B. Wang, H. Liu and J. Yao, The Journal of Physical Chemistry C, 2008, 112, 8192-8195.
21. Y. Si and E. T. Samulski, Nano Letters, 2008, 8, 1679-1682.
22. M. Zhou, Y. Wang, Y. Zhai, J. Zhai, W. Ren, F. Wang and S. Dong, Chemistry – A European Journal, 2009, 15, 6116-6120.
23. H. C. Schniepp, J.-L. Li, M. J. McAllister, H. Sai, M. Herrera-Alonso, D. H. Adamson, R. K. Prud'homme, R. Car, D. A. Saville and I. A. Aksay, The Journal of Physical Chemistry B, 2006, 110, 8535-8539.

24. Y. Zhu, S. Murali, M. D. Stoller, A. Velamakanni, R. D. Piner and R. S. Ruoff, Carbon, 2010, 48, 2118-2122.
25. L. J. Cote, R. Cruz-Silva and J. Huang, Journal of the American Chemical Society, 2009, 131, 11027-11032.
26. I. Roppolo, A. Chiappone, K. Bejtka, E. Celasco, A. Chiodoni, F. Giorgis, M. Sangermano and S. Porro, Carbon, 2014, 77, 226-235.
27. G. Fanchini and A. Tagliaferro, Journal of Non-Crystalline Solids, 2006, 352, 1319-1322.
28. M. Rovere, S. Porro, S. Musso, A. Shames, O. Williams, P. Bruno, A. Tagliaferro and D. M. Gruen, Diamond and Related Materials, 2006, 15, 1913-1916.
29. A. I. Shames, A. M. Panich, S. Porro, M. Rovere, S. Musso, A. Tagliaferro, M. V. Baidakova, V. Y. Osipov, A. Y. Vul, T. Enoki, M. Takahashi, E. Osawa, O. A. Williams, P. Bruno and D. M. Gruen, Diamond and Related Materials, 2007, 16, 1806-1812.
30. S. Musso, S. Porro, M. Rovere, A. Tagliaferro, E. Laurenti, M. Mann, K. B. K. Teo and W. I. Milne, Diamond and Related Materials, 2006, 15, 1085-1089.
31. S. S. Rao, A. Stesmans, K. Keunen, D. V. Kosynkin, A. Higginbotham and J. M. Tour, Applied Physics Letters, 2011, 98, -.
32. S. S. Rao, A. Stesmans, J. van Tol, D. V. Kosynkin, A. Higginbotham-Duque, W. Lu, A. Sinitskii and J. M. Tour, ACS Nano, 2012, 6, 7615-7623.
33. H. Ma, R. H. Davis and C. N. Bowman, Macromolecules, 1999, 33, 331-335.
34. J. J. Park, D. M. Park, J. H. Youk, W. R. Yu and J. Lee, Carbon, 2010, 48, 2899-2905.
35. J. R. Nair, A. Chiappone, C. Gerbaldi, V. S. Ijeri, E. Zeno, R. Bongiovanni, S. Bodoardo and N. Penazzi, Electrochimica Acta, 2011, 57, 104-111.
36. C. Decker, Progress in Polymer Science, 1996, 21, 593-650.
37. D. A. Shirley, Physical Review B, 1972, 5, 4709-4714.
38. M. Sangermano, A. Tagliaferro, D. Foix, M. Castellino and E. Celasco, Macromolecular Materials and Engineering, 2014, 299, 757-763.
39. J. R. Nair, A. Chiappone, C. Gerbaldi, V. S. Ijeri, E. Zeno, R. Bongiovanni, S. Bodoardo and N. Penazzi, Electrochimica Acta, 2011, 57, 104-111.
40. X. L. Hou, J. L. Li, S. C. Drew, B. Tang, L. Sun and X. G. Wang, Journal of Physical Chemistry C, 2013, 117, 6788-6793.
41. Y. Morita, S. Suzuki, K. Sato and T. Takui, Nature Chemistry, 2011, 3, 197-204.
42. E. G. Janzen and J. I. P. Liu, Journal of Magnetic Resonance (1969), 1973, 9, 510-512.
43. K. Makino, A. Hagi, H. Ide, A. Murakami and M. Nishi, Canadian Journal of Chemistry, 1992, 70, 2818-2827.
44. C. E. Diaz-Uribe, M. C. Daza, F. Martínez, E. A. Páez-Mozo, C. L. B. Guedes and E. Di Mauro, Journal of Photochemistry and Photobiology A: Chemistry, 2010, 215, 172-178.
45. D. R. Duling, Journal of Magnetic Resonance, Series B, 1994, 104, 105-110.